ROCK CLASSIFICATION VIA TRANSFER LEARNING IN THE SCOPE OF CHEMCAM RMI IMAGE DATA Ana Lomashvili[1], Alexander von Canal[1], Kristin Rammelkamp[1]; [1]German Aerospace Center (DLR), Institute of Optical Sensor Systems, Berlin, Germany; ana.lomashvili@dlr.de

Introduction: NASA's Mars Science Laboratory (MSL) rover Curiosity is equipped with the ChemCam instrument suite to analyze chemical composition of rocks and soils in Gale crater [1, 2]. The instrument consists of two components: the first planetary science Laser-Induced Breakdown Spectrometer (LIBS) and a Remote Micro-Imager (RMI) [3]. The LIBS instrument, composed of a powerful laser and spectrometers, provides elemental composition of rocks and soil at the surface of Mars [4]. The RMI images through the same telescope as the LIBS providing context to the samples. The RMI dataset consists of images taken before and after the LIBS measurements. As small portions of sample material are ablated with each LIBS measurement, the post-LIBS images can show small ($\approx 500\,\mu$m) craters depending on sample properties, e.g. rock hardness [3]. The instrument pictured approximately more than 3000 targets and collected LIBS spectra from multiple points of each target (5-25 points per target). This study is focused on classifying rock types and soils based on RMI images, thus on visual characteristics such as texture, grain sizes etc. In a previous study, attributes corresponding to rock facies were assigned to RMI images resulting in 17-digit binary strings for each target. These were then used to group similar targets together [5, 6]. In this work, the RMI images are used directly as input for methods from the field of machine learning to first explore the unlabeled data and group similar types of rocks together. In the second step, the results are used to label data and train a classification model.

Dataset: The images for this study are retrieved from *PDS Geosciences node* [7]. We selected only those images showing the context of LIBS measurements. For each LIBS target, there are two RMI images: before and after the LIBS measurement. Inputting the images with the LIBS craters would force the model to learn traces of the LIBS measurements and group them accordingly. Although the appearance of LIBS craters provides additional information about the target, we decided to focus in this study on the visual characteristics of the samples. Therefore, only images before the LIBS measurements were picked. We have scrapped a total of 2700 images from sol 1000 to sol 3300. The original image size is 1200×1200 pixels. We have cropped and resized the images to accelerate the model and ended up with 128×128 pixel images. These steps shortlist and prepare data for the further exploration.

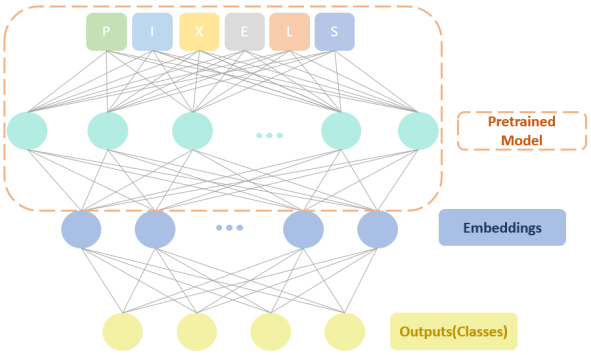

Figure 1: *Schematic representation of a transfer learning model showing the creation of embbedings by freezing the layers in the dashed box.*

Methods: In order to get familiarized with the broad range of unlabeled targets, one of the options is to apply unsupervised learning. Despite taking a few preprocessing steps in the previous section, there is still a need for additional data preparation to better expose the underlying patterns to algorithms. As an input feeding raw data to a model groups the images according to their pixel values. Although such approach works when the intention is color segmentation of the image, our prime goal is to cluster the images according to their texture, grain size, contours, etc [8]. Therefore, we use *Transfer learning* to extract features from the images and cluster them accordingly. Transfer learning, as the name suggests, passes knowledge of one model to another which will be explained in the following. Figure 1 illustrates a simple neural network architecture with inputs of pixel values, 5 outputs, and 2 hidden layers. The layer before the last one is able to capture all the information from the input image. These nodes, providing representation of the input, are called embeddings. Embeddings are created by applying a set of mathematical operations to the input image. In the case of lacking enough training dataset, one can repurpose the embedding creation part from a model that has been trained on a much larger dataset. By getting rid of the last layer that classifies input data into specific classes, one can replace it with desired classes. In this way, a model trained on a large dataset is repurposed to classify different data. Here, we have used this approach to create embeddings as an additional preprocessing step [9]. As a pretrained model, the Inception-v3 is used, which was trained for the ImageNet "Large Visual Recognition Challenge". The original data contains millions of images corresponding to 1000 classes [10].

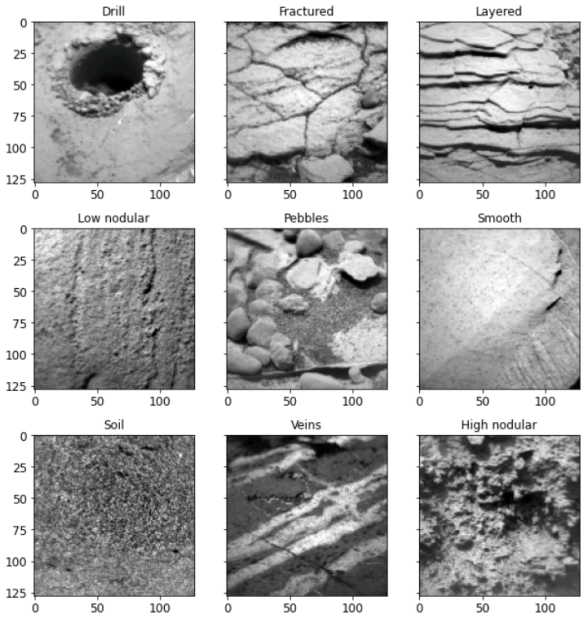

Figure 2: *RMI images of representative targets for each of the identified 9 classes.*

The wide variety of images provides useful embeddings for our dataset.

The extracted features are fed to an unsupervised technique, *K-means* clustering. On the very first iteration, the algorithm randomly chooses centroids, i.e. representative samples, and assigns the closest instances to them. Iteratively, the centroids and labels are updated until the algorithm converges. In this manner, the method allows grouping similar instances together into clusters. The drawback of the algorithm is that it requires setting the number of clusters beforehand. To find this number, we use the *Silhouette scores* which is a measure of cluster quality as it portrays how well the instances reside within their clusters [8]. The silhouette score plot and visual inspection of clusters helped us decide to categorize the dataset into 9 classes.

Data labeling: We initiated the labeling process by analyzing 50 images from the dataset. This subset of images was chosen using k-means clustering instead of randomly picking the samples. The algorithm grouped all the images with a total number of 50 clusters. The choice of the number of clusters was made for labeling purposes. The representative images of the clusters were picked for review. Such an approach guarantees to have as diverse images as possible that is beneficial for semi-supervised learning. Following are the labels: drill, fractured, layered, low nodular, pebbles, smooth, soil, veins, high nodular. Low and high nodular rocks are different in size of nodules. Figure 2 illustrates labels and corresponding RMI images.

Classification: As mentioned above, we have categorized the 50 samples into 9 classes. As we are dealing with a small set of samples, 2700 images in total, training a classification model from scratch would result in overfitting: As a rule of thumb, at least 1000 samples are needed per label [9]. Therefore, we again applied transfer learning by using the 50 labeled images in semi-supervised learning. Additionally, we manually labeled more images according to the 9 classes identified in the first step. Finally we used 100 images per class to avoid dealing with an unbalanced set of input data. Once more we adopted embeddings from the Inception-v3 pretrained model for the training. Although further improvements are needed, the preliminary classification model shows promising results which will be detailed in a future work.

Challenges: The very first issue, we were facing is the lack of labeled data. The labeling will be continued and data augmentation will be employed. The second challenge is inconsistency in the data that is caused by: image quality, illumination.

Although we have removed outliers, still there might be, e.g., out of focus images that contribute to reduced model accuracy. Moreover, as the images are taken during different time periods the illumination changes.

Future plans: Our next step is to augment the existing data and enhance the current classification method. The final goal is to fuse LIBS and RMI data to improve the classification accuracy of rocks based on both visual characteristics and geochemical composition.

References: **[1]** Wiens et al. "The ChemCam Instrument Suite on the Mars Science Laboratory (MSL) Rover: Body Unit and Combined System Tests". In: *SSR* 170 (2012). **[2]** Maurice et al. "The ChemCam Instrument Suite on the Mars Science Laboratory (MSL) Rover: Science Objectives and Mast Unit Description". In: *SSR* 170 (2012). **[3]** Mouélic et al. "The ChemCam Remote Micro-Imager at Gale crater: Review of the first year of operations on Mars". In: *Icarus* 249 (2015). **[4]** Cremers et al. *Handbook of Laser-Induced Breakdown Spectroscopy*. 2006. **[5]** Essunfeld et al. "Attribute recognition for grouping elevated-manganese ChemCam targets by visual characteristics". In: *52nd LPCS* (2021). **[6]** Essunfeld et al. "Grouping ChemCam targets by visual characteristics improved by automatic partitioning". In: *53rd LPCS* (2022). **[7]** R Wiens. *MSL ChemCam Remote Micro- Imaging Camera raw data*. MSL-M-CHEMCAM-RMI-2-EDR-V1.0, NASA Planetary Data System. 2013. **[8]** A. Géron. *Hands-On ML with Scikit-Learn, Keras, and TF*. Third. 2022. **[9]** Lakshmanan et al. *Practical ML for Computer Vision*. 2021. **[10]** Szegedy et al. "Rethinking the Inception Architecture for Computer Vision". In: *IEEE CCVPR* (2016).